THROMBOSIS AND HEMOSTASIS

von Willebrand factor fibers promote cancer-associated platelet aggregation in malignant melanoma of mice and humans

Alexander T. Bauer,[1] Jan Suckau,[1] Kathrin Frank,[2] Anna Desch,[1] Lukas Goertz,[1] Andreas H. Wagner,[3] Markus Hecker,[3] Tobias Goerge,[4] Ludmila Umansky,[5] Philipp Beckhove,[5] Jochen Utikal,[2] Christian Gorzelanny,[1] Nancy Diaz-Valdes,[2,6] Viktor Umansky,[2] and Stefan W. Schneider[1]

[1]Experimental Dermatology, Medical Faculty Mannheim, University of Heidelberg, Mannheim, Germany; [2]Skin Cancer Unit, German Cancer Research Center (DKFZ), Heidelberg and Department of Dermatology, Venereology and Allergology, University Medical Center Mannheim, Ruprecht-Karl University of Heidelberg, Mannheim, Germany; [3]Institute of Physiology and Pathophysiology, University of Heidelberg, Heidelberg, Germany; [4]Department of Dermatology, University of Muenster, Muenster, Germany; [5]Department of Translational Immunology, German Cancer Research Center (DKFZ), Heidelberg, Germany; and [6]Division of Hepatology and Gene Therapy, Center for Applied Medical Research, University of Navarra, Pamplona, Spain

Key Points

- Tumor-derived VEGF-A mediates endothelial cell activation, VWF release, and platelet aggregation provoking coagulation in tumor patients.
- Local ADAMTS13 inhibition promotes VWF fiber formation in tumor microvessels.

Tumor-mediated procoagulatory activity leads to venous thromboembolism and supports metastasis in cancer patients. A prerequisite for metastasis formation is the interaction of cancer cells with endothelial cells (ECs) followed by their extravasation. Although it is known that activation of ECs and the release of the procoagulatory protein von Willebrand factor (VWF) is essential for malignancy, the underlying mechanisms remain poorly understood. We hypothesized that VWF fibers in tumor vessels promote tumor-associated thromboembolism and metastasis. Using in vitro settings, mouse models, and human tumor samples, we showed that melanoma cells activate ECs followed by the luminal release of VWF fibers and platelet aggregation in tumor microvessels. Analysis of human blood samples and tumor tissue revealed that a promoted VWF release combined with a local inhibition of proteolytic activity and protein expression of ADAMTS13 (a disintegrin-like and metalloproteinase with thrombospondin type I repeats 13) accounts for this procoagulatory milieu. Blocking endothelial cell activation by the low-molecular-weight heparin tinzaparin was accompanied by a lack of VWF networks and inhibited tumor progression in a transgenic mouse model. Our findings implicate a mechanism wherein tumor-derived vascular endothelial growth factor-A (VEGF-A) promotes tumor progression and angiogenesis. Thus, targeting EC activation envisions new therapeutic strategies attenuating tumor-related angiogenesis and coagulation. (*Blood*. 2015;125(20):3153-3163)

Introduction

To form new metastatic lesions, circulating melanoma cells have to interact with endothelial cells (ECs) and migrate through the vessel wall.[1,2] In this context, our own in vitro studies show that melanoma cells activate ECs by an indirect, tissue factor (TF)–mediated thrombin generation.[3] Next to this indirect melanoma-induced EC activation, recent findings identified melanoma-derived vascular endothelial growth factor-A (VEGF-A) as main mediator of direct EC activation.[4,5] Both the thrombin- and the VEGF-A–dependent pathways induce EC activation followed by Weibel-Palade body (WPB) exocytosis and the release of inflammatory cytokines and the highly procoagulatory glycoprotein von Willebrand factor (VWF), linking inflammation and coagulation.[6] On the one hand, luminally released VWF fibers are involved in hemostasis and vessel repair as mediators of platelet adhesion to the endothelium.[7,8] On the other hand, we showed that tumor cell-induced ultra-large VWF (ULVWF) fibers have the highest potential for platelet binding and aggregation.[9,10] This effect may contribute not only to pathophysiologic vessel occlusion,[11] but also to the establishment of metastasis as platelets facilitate tumor cell extravasation.[12-14]

Indeed, it is well-known that cancer patients hold a high risk of thromboembolism associated with an enhanced incidence of metastasis and a decrease of overall survival.[15-17] Especially in malignant melanoma patients, the incidence of venous thromboembolism (VTE) is ~25%.[18] Moreover, clinical studies demonstrate that treatment with anticoagulant low-molecular-weight heparins (LMWHs) improves the outcome of distinct cancer patients.[19] Based on these observations, we postulate that EC activation, followed by the generation of VWF fibers in tumor vasculature, promotes cancer-associated hypercoagulopathy and facilitates metastasis.

Here, we demonstrate the existence of VWF fibers mediating platelet aggregation within tumor microvessels in 2 different tumor mouse models and in human tumor tissue promoted by an increased EC activation and a local inhibition of the VWF-degrading enzyme ADAMTS13 (a disintegrin-like and metalloproteinase with

Submitted August 14, 2014; accepted February 3, 2015. Prepublished online as *Blood* First Edition paper, February 24, 2015; DOI 10.1182/blood-2014-08-595686.

A.T.B. and J.S. contributed equally to this work.

The online version of this article contains a data supplement.

There is an Inside *Blood* Commentary on this article in this issue.

The publication costs of this article were defrayed in part by page charge payment. Therefore, and solely to indicate this fact, this article is hereby marked "advertisement" in accordance with 18 USC section 1734.

thrombospondin type I repeats 13). Binding and inhibition of tumor-derived VEGF-A by the LMWH tinzaparin blocked EC activation, thereby attenuating VWF fiber formation on the luminal surface of ECs. Finally, treatment with tinzaparin impaired VWF network formation and led to reduced tumor growth, tumor angiogenesis, and a suppression of metastasis in a *ret* transgenic mouse model spontaneously developing melanomas.[20] Our study provides new insights into the crucial role of the vascular endothelium promoting both tumor-associated coagulation and metastasis.

Methods

Mouse procedures

All experiments were approved by the governmental animal care authorities. *Ret* transgenic mice[21,22] developing skin melanoma spontaneously were treated with tinzaparin 0.6 IU/g (innohep; Leo Pharma) or NaCl subcutaneously. Details are provided in the supplemental Methods (see supplemental Data available at the *Blood* Web site).

Human malignant melanoma tissue

Informed written consent was obtained from all participants in accordance with the Declaration of Helsinki and the International Conference on Harmonization of Technical Requirements for Registration of Pharmaceuticals for Human Use (ICH) guidelines. The protocol received approval from the ethics committee of the Medical Faculty Mannheim, Heidelberg University (Germany; 2010-318N-MA). Patients with malignant melanoma stage UICC III and IV were selected from the Department of Dermatology, Venereology and Allergology, Heidelberg.

Immunofluorescence analysis

Cryosections (10 μm) were incubated with the following primary antibodies: rabbit anti-human VWF (DakoCytomation), rat anti-mouse CD42b (emfret Analytics), mouse anti-human Thrombospondin (Laboratory Vision/Neomarkers), mouse anti-human CD31 (DakoCytomation), rat anti-mouse CD31 (BD Biosciences), Ki67–fluorescein isothiocyanate (FITC) (BD Biosciences), rabbit anti-VEGF-A (Santa Cruz Biotechnology). The following secondary antibodies were used: FITC-conjugated goat anti-rabbit (BD Pharmingen), Alexa 555–conjugated goat anti-rat immunoglobulin G (IgG; Invitrogen), or Alexa 555–conjugated goat anti-mouse. Nuclei were stained with 4,6 diamidino-2-phenylindole (DAPI) and microscopy was performed using an Axiovert 200 microscope (Zeiss). Images were processed with AxioVision software (4.8) and ImageJ (1.47c).

Bio-plex assay

Snap-frozen melanoma samples were mechanically disrupted and treated with lysis solution (Bio-Rad). After sonication, samples were centrifuged (4500*g*; 10 minutes; 4°C). Protein concentration was determined using the Pierce BCA protein assay kit (Thermo Scientific) and adjusted to 1000 μg/mL using serum diluent (Bio-Rad). Protein concentrations in tissue lysates were measured by multiplex technology (Bio-Rad). Bio-plex assays for in vitro studies can be found in the supplemental Methods.

ADAMTS13 activity measurements

ADAMTS13 activity was measured in citrate plasma by a commercially available kit according to the instructions of the manufacturer (Technoclone GmbH). In tissue lysates (1% Triton X-100 in phosphate-buffered saline [PBS]), ADAMTS13 activity was measured using FRETS-VWF73 (American Diagnostica).

Western blot

Tumor tissue and skin were homogenized (1% Triton X-100 in PBS) and protein concentration was quantified using the Bradford assay. In total, 40 μg of protein was separated by sodium dodecyl sulfate–polyacrylamide gel electrophoresis (SDS-PAGE) and western blot was performed according to standard protocols using a polyclonal antibody to ADAMTS13 (Santa Cruz Biotechnology) for detection.

ELISA techniques

Secretion of VWF was quantified using a sandwich enzyme-linked immunosorbent assay (ELISA) technique as described before.[3] ELISA for VEGF-A was performed in accordance with the instructions of the manufacturer (Bender MedSystems).

Flow cytometry

Single-cell suspension of fresh tumor tissue and lymph nodes was produced as described before.[23] Cell suspensions were treated with Fc-block and antibodies for 20 minutes at 4°C. To exclude leukocytes and identify melanoma cells, cells were incubated with primary anti-mouse antibodies (CD45.2-PerCP-Cy5.5; mouse anti-human Ki67-Fitc; BD Biosciences) for 1 hour. Acquisition was done using FACSCanto II with FACSDiva software (both BD Biosciences). FlowJo software (Tree Star) was used for analysis of at least 100 000 events. Data were expressed as histograms.

In vitro studies

Stimulation of endothelial cells. Generation of Ret melanoma-derived supernatants and stimulation of human umbilical vein endothelial cells (HUVECs) were performed as described before.[3] Briefly, melanoma supernatants were used with or without addition of bevacizumab (0.65 mg/mL; Roche), tinzaparin (100 IU/mL, innohep; Leo Pharma) for stimulation. Details are provided in the supplemental Methods.

RNA preparation and reverse transcription quantitative polymerase chain reaction. Total RNA was extracted using the RNeasy mini kit (Qiagen GmbH) as described before.[4] Details are provided in the supplemental Methods.

Fluorescence spectroscopic analysis of the VEGF-tinzaparin interaction. To measure VEGF-tinzaparin interaction, we added tinzaparin (concentration range, 5 μM to 80 μM) to 0.5 μM human recombinant VEGF-A (R&D Systems) in PBS. The reaction mixtures were incubated at room temperature for 20 minutes and measured in a fluorescence spectrometer (excitation, 290 nm; emission, 320-450 nm; Tecan infinite M200, Tecan Group Ltd.). The pentasaccharide fondaparinux was used as control. K_d values were calculated with GraphPad Prism using a 1-site specific nonlinear regression analysis.

ATP quantification. Cellular adenosine triphosphate (ATP) levels were assessed using the CellTiter-Glo luminescent cell viability assay according to the manufacturer (Promega). A detailed description is provided in the supplemental Methods.

Statistical analysis

Significance was tested by Student *t*/Mantel-Cox testing using GraphPad Prism (version 6.0). Error bars show the standard error of the mean and $*P < .05$ was considered as significant difference.

Results

Tumor micromilieu promotes VWF fiber formation

To investigate the role of tumor-mediated EC activation in vivo, we analyzed the distribution of VWF in vessels of primary skin tumors of *ret* transgenic mice characterized by spontaneous melanoma development and metastasis similar to the clinical situation.[20] VWF, stored in WPBs, showed a typical punctate staining in the vessel wall of healthy control skin and virtually no VWF within the vessel lumen (Figure 1A-B arrowheads). By contrast, in tumor tissue a clear decrease in VWF abundance was detected in the cytoplasm of

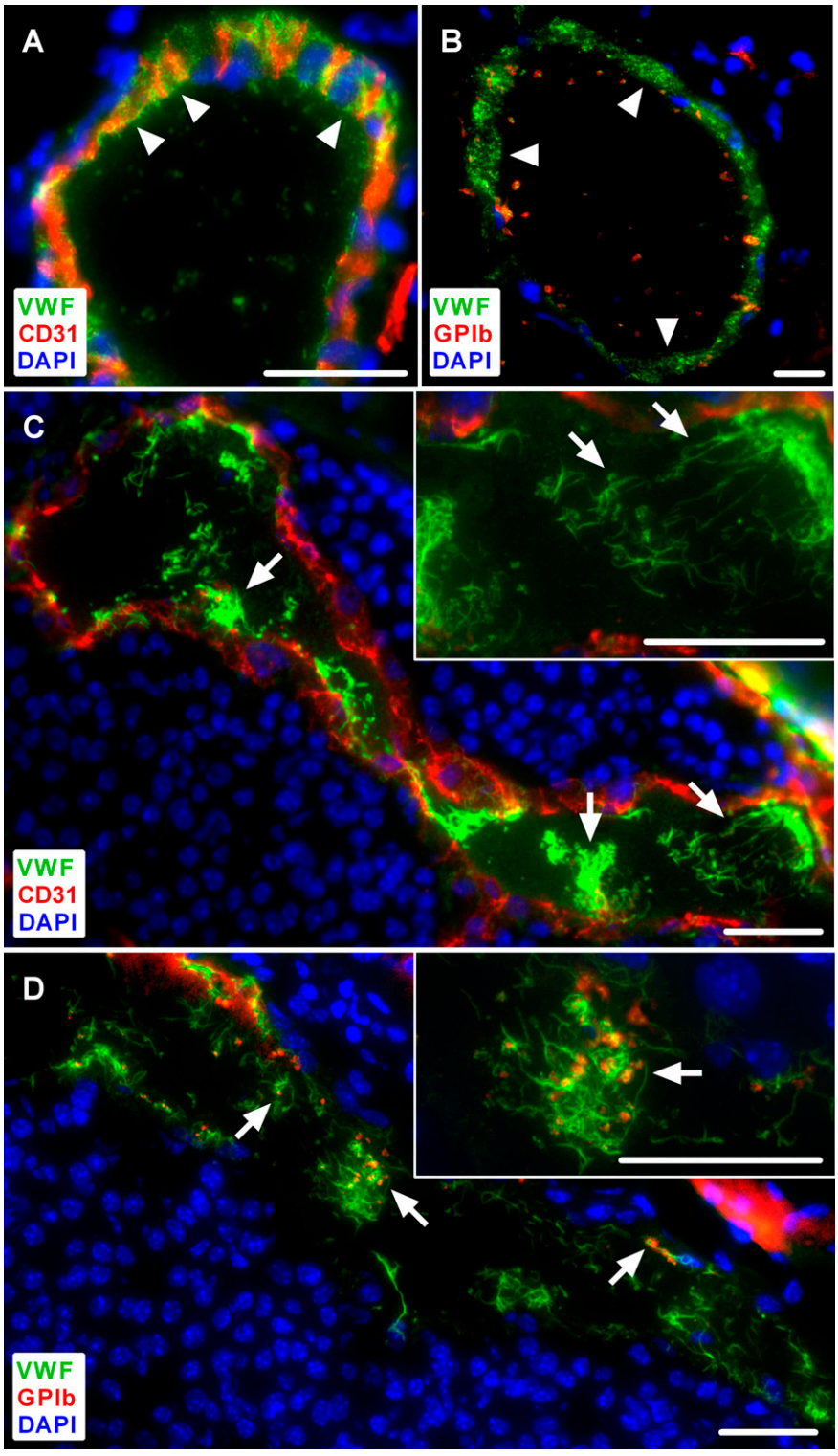

Figure 1. Immunofluorescence analysis of tumor microvessels compared with healthy control skin in *ret* transgenic mice. Cryosections were stained for VWF and CD31 (A,C). An anti-GPIb antibody was used to identify platelets (B,D). Nuclei were stained with DAPI. Representative images of control skin show VWF localized within the vessel wall, lacking ULVWF fibers within the lumen (A-B, arrowheads) and only few platelets are visible (B, red). By contrast, in tumor microvessels, ULVWF fibers are detectable within the vessel lumen indicating EC activation (C, arrows). These ULVWF fibers bind platelets as shown in the same vessel (D, red, arrows). Insets, A higher magnification of the presented images (n = 4 to 10 animals; scale bars = 20 μm). See also supplemental Figures 1-2.

the ECs indicative of EC activation (Figure 1C-D). WPB exocytosis was confirmed by an increased formation of ULVWF fibers within tumor blood vessels (Figure 1C arrows). We found clearly visible ULVWF fibers (defined as ULVWF fibers ≥5 μm) in 32.9% of all tumor vessels, but only in 8.0% of all analyzed vessels in control tissue of nontransgenic littermates (supplemental Table 1).

Because VWF is an effective binding partner for circulating platelets, we assumed that melanoma cell-mediated EC activation may result in platelet aggregation. As expected, there was almost no platelet recruitment to the nonactivated endothelium of the control skin (Figure 1B). However, platelet aggregates and adhesion to ECs were clearly visible in the tumor vasculature and seemed to be dependent on the presence of ULVWF fibers on the luminal surface of the vessel wall (Figures 1D arrows; supplemental Figure 1). In addition, we detected in some microvessels an occluding thrombotic clot mainly consisting of VWF and platelets resembling the kind of microvessel occlusion prototypic for patients with thrombotic thrombocytopenic purpura (TTP; supplemental Figure 2). Therefore, the ULVWF fibers in

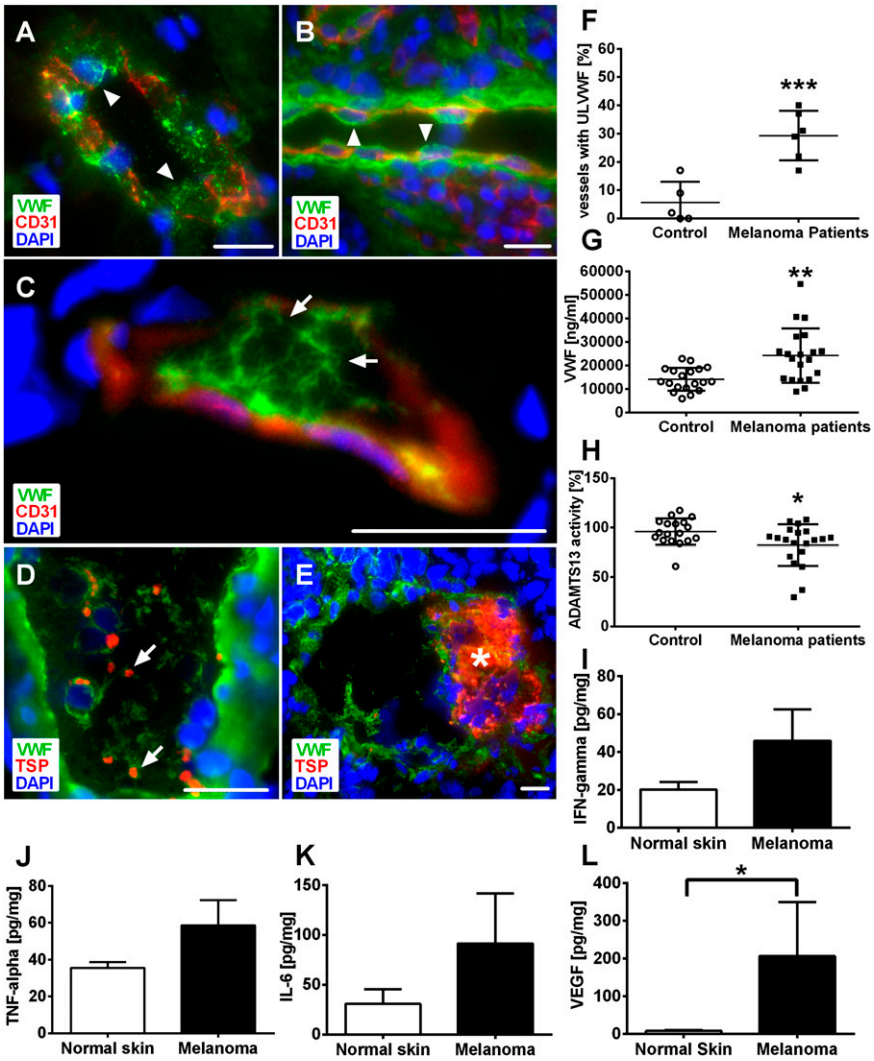

Figure 2. Local inhibition of ADAMTS13 promotes VWF fiber formation in microvessels obtained from human melanoma patients. Cryosections of human malignant melanoma tissue, healthy control skin, and basal cell carcinoma were analyzed by immunofluorescence stainings for VWF and CD31 (A-C) or thrombospondin (TSP) (D-E). Nuclei were stained with DAPI. Analysis of healthy skin (A) and human basal cell carcinoma (B) as control demonstrate storage of VWF in the vessel wall (arrowheads). ULVWF fibers are detected in the lumen of the microvessels, correlating to reduced VWF within the vessel wall indicative of EC activation (C, arrows). These ULVWF fibers bind platelets (D, arrows) and are associated with microthrombi formation in distinct microvessels (E, asterisk; n = 5 to 6; scale bars = 20 μm). Quantification showed significantly increased numbers of vessels with luminal VWF fibers in tumor vasculature compared with healthy skin (F). Systemic VWF level in blood samples of malignant melanoma patients was increased compared with healthy control (G). By contrast, only a slight reduction of ADAMTS13 activity was observed (H). Tumor-derived cytokines and growth factors were measured in healthy control skin and tumor of human malignant melanoma by bio-plex. Cytokine levels of IFN-γ (I), TNF-α (J), and IL-6 (K) were increased in tumor samples compared with control skin. The concentration of VEGF-A was significantly increased within melanoma compared with control (L). Results of 9 different melanoma patients are shown (*$P < .05$, **$P < .005$, ***$P < .001$). Bars indicate the mean ± SD.

the lumen of microvessels indicate an intrinsic stimulation by the tumor and/or stroma cells in the spontaneously developed melanomas.

ULVWF fibers are generated within microvessels of human malignant melanoma patients

To prove the clinical significance of these findings, we evaluated cryosections of human malignant melanoma tissue obtained from 6 patients (supplemental Table 1; Figure 2C-F). We identified, in 29.3% of all microvessels, intraluminal ULVWF fibers (Figure 2F arrows; supplemental Table 1). In contrast, microvessels from tissue of human basal cell carcinoma (nonmetastatic, semimalignant tumor) or control skin displayed a localization of VWF solely within the ECs lacking any ULVWF fibers within the vessel lumen (supplemental Table 1; Figure 2A-B arrowheads). In line with our animal data, blood vessels in human melanomas were characterized by strong EC activation, the formation of ULVWF fibers (Figure 2C-D arrows), platelet binding (Figure 2D arrows), and microthrombus formation (Figure 3E asterisk).

Systemic ADAMTS13 baseline activity indicates local inhibition of ADAMTS13 in tumor microvessels

The observations described in the previous sections strongly suggest that the formation of tumor ULVWF networks is due to a loss of ADAMTS13 activity and enhanced EC activation associated with an imbalance of VWF release and degradation.

To examine the underlying mechanisms, we measured the systemic level of VWF from patients suffering from malignant melanoma. The mean serum level of VWF was 24 239 ng/mL ± 11 544 ng/mL in cancer patients, almost twofold increased compared with 14 077 ng/mL ± 4910 ng/mL in healthy controls (Figure 2G; $P < .005$). Furthermore, we quantified the ADAMTS13 activity in serum samples (Figure 2H). In healthy controls, mean ADAMTS13 activity was 95.92% ± 13.28% (n = 18) and was decreased to 82.32% ± 20.96% (n = 20) in melanoma patients. Therefore, the measured systemic activity of ADAMTS13 is clearly within the range required to maintain a physiological equilibrium of ULVWF fiber formation and degradation because the latter has been shown to break down only at enzyme activities around 5% to 20% and below.[24,25]

Next, to analyze local changes of ADAMTS13 activity in tumor microvessels, we measured interleukin-6 (IL-6), tumor necrosis factor-α (TNF-α), IL-4, and interferon-γ (IFN-γ) in melanoma metastasis samples from 9 patients by bio-plex assay because these cytokines have been shown to decrease ADAMTS13 activity.[26,27] In line, all cytokines were clearly increased in human tumor samples (except IL-4, showing only a slight increase; data not shown) compared with healthy skin (Figure 2I-K).

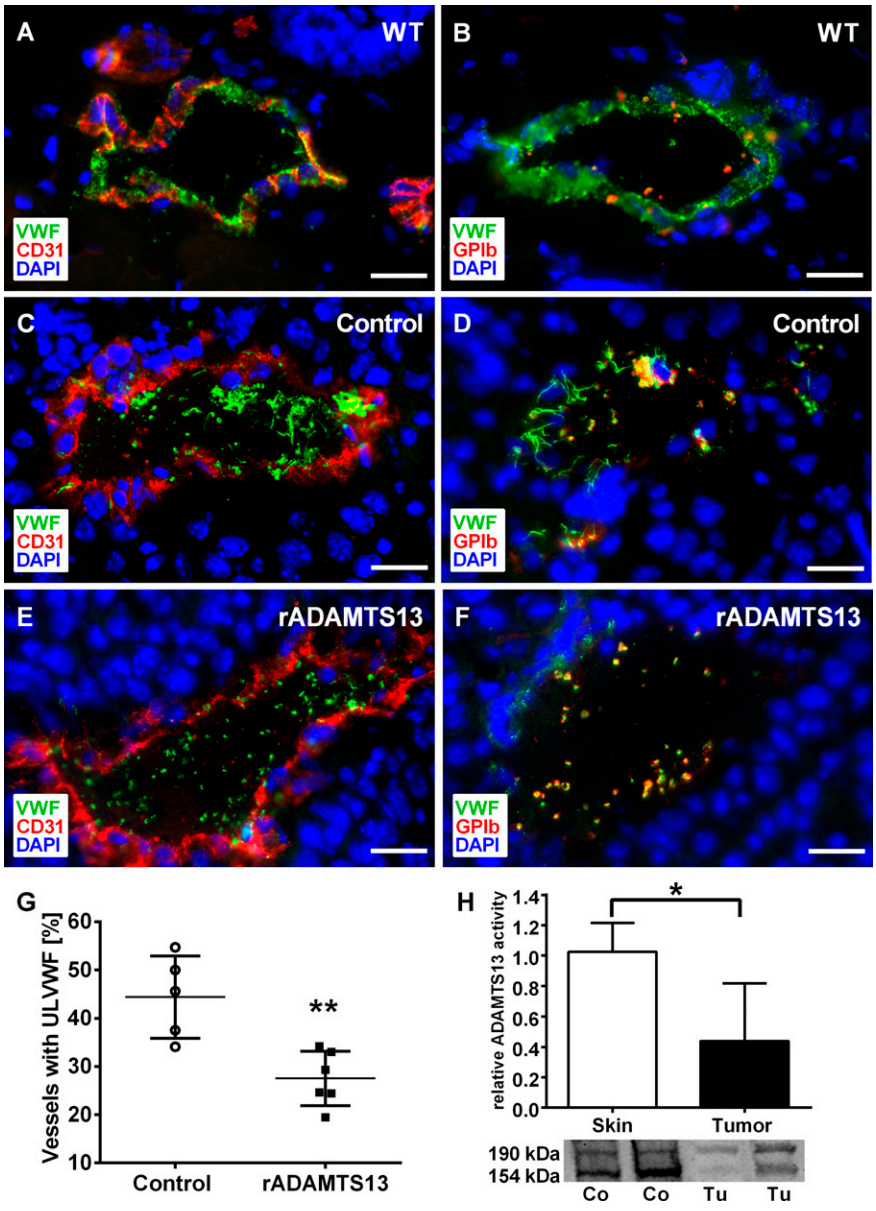

Figure 3. Reduced ADAMTS13 activity in tumor tissue promotes intraluminal VWF fiber formation in tumor microvessels. Immunofluorescence staining of cryosections for VWF (green), platelets (red), and the endothelial cell marker CD31 (red). DNA was stained with DAPI (blue). Mouse melanoma cells (Ret) were injected intradermally and mice were treated with recombinant ADAMTS13 (rADAMTS13; E-F) or 0.9% NaCl (C-D) as control. Reconstitution of ADAMTS13 reduced the formation of intraluminal ULVWF networks and platelet aggregation compared with vehicle treatment. In comparison with wild-type skin (A-B), less VWF in the vessel wall indicates ULVWF degradation after exocytosis (n = 5-6 animals; scale bars = 20 μm). To analyze the impact of ADAMTS13 on VWF fiber formation, vessels with or without luminal fibers were quantified. Infusion with rADAMTS13 significantly decreased the number of vessels with ULVWF (G). The activity and the protein expression of ADAMTS13 in tumor tissue were significantly reduced compared with healthy skin measured by a FRET-based assay and western blot (H; n = 3-5 animals, $*P < .05$, $**P < .005$). See also supplemental Table 2.

As mentioned previously, a lack of ADAMTS13 activity alone is not sufficient and a marked EC activation is also needed to induce ULVWF fiber formation. Because VEGF is a potent activator of human ECs,[4] we measured its concentration in human melanomas. As shown in Figure 2L, VEGF-A was significantly increased within the tumors compared with control tissue and thereby may account for the observed EC activation and ULVWF release.

Reduced ADAMTS13 activity promotes ULVWF fiber formation in tumor vessels

To analyze whether recombinant ADAMTS13 in the peripheral blood could rescue the localized inhibition of ADAMTS13 activity, we applied a second mouse model, based on intradermal inoculation of melanoma cells (Figure 3).

Comparable to previous results, 44.4% of the tumor microvessels of vehicle-treated control mice exhibited ULVWF fibers (Figure 3G; supplemental Table 2). IV infusion of recombinant ADAMTS13 reduced luminal ULVWF fiber formation significantly to 27.5% in tumor-bearing mice. We concluded VWF network degradation after luminal VWF release because VWF detected in the vessel wall was reduced compared with healthy controls (Figure 3E-F).

Moreover, we found a strong reduction of the proteolytic activity of ADAMTS13 in tumor tissue compared with healthy skin using a new in situ activity assay (Figure 3H). We next analyzed the protein expression of ADAMTS13 in the tissue by western blot analysis. The antibodies against ADAMTS13 recognized bands with molecular weights of about 154 and 190 kDa indicating differentially processed protein isoforms. For both bands, tumor tissue exhibited reduced protein levels compared with skin (Figure 3H). Therefore, data provide evidence for reduced ADAMTS13 activity within tumor microvessels.

Tinzaparin blocks Ret cell-induced EC activation in vitro via binding to VEGF-A

To resolve the molecular mechanisms of EC activation mediated by mouse melanoma cells, we incubated ECs with the supernatant of the melanoma cell line Ret established from skin tumors developing in

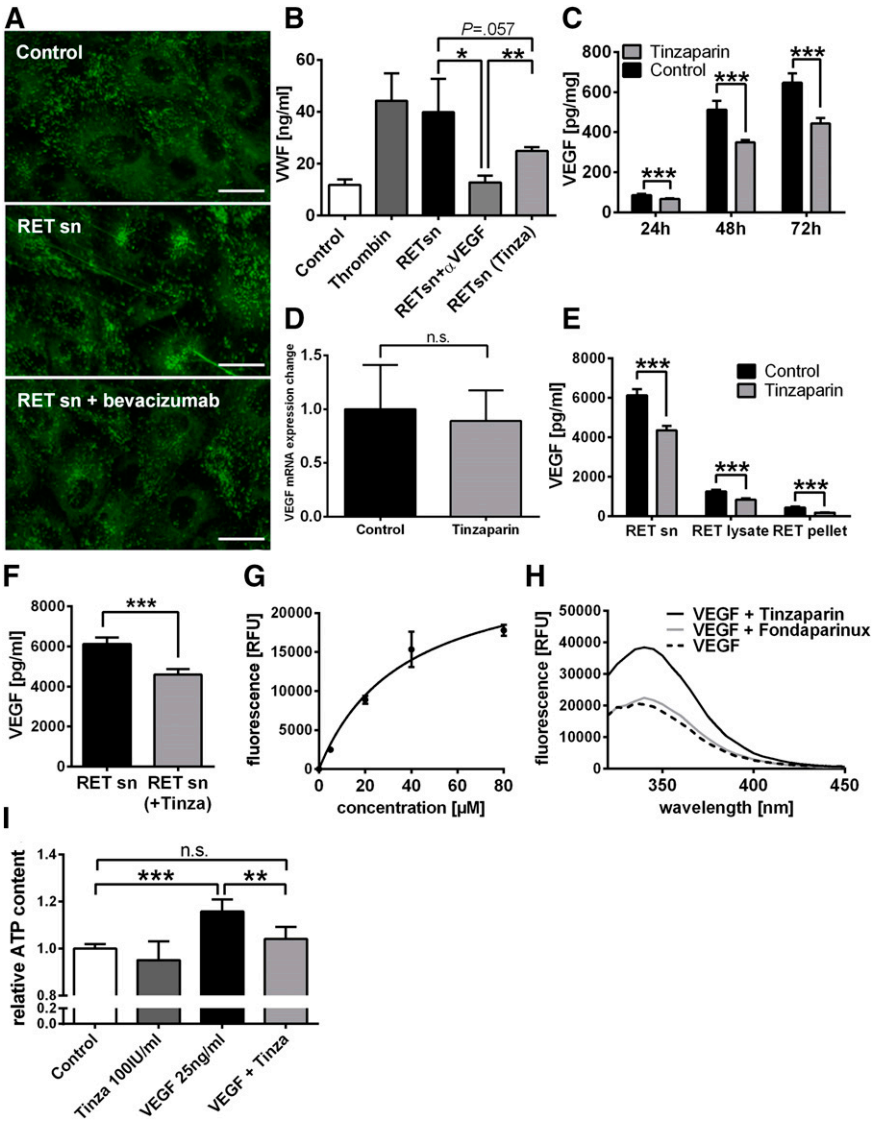

Figure 4. The melanoma cell line Ret induces endothelial cell stimulation via VEGF-A. HUVECs were stimulated for 15 minutes with the supernatant (sn) of the melanoma cell line *Ret* alone or supplemented with 0.65 mg/mL bevacizumab and thrombin (0.5 IU/mL) was used as a positive control. The efficiency of the melanoma cell-induced EC stimulation was quantified by measurement of VWF release by immunofluorescence staining (A) and by ELISA for VWF (B). Supplementation of Ret cells with bevacizumab or tinzaparin (100 IU/mL) reduced tumor cell-induced VWF release (B). Measurement of VEGF-A revealed that incubation with tinzaparin for 24 hours, 48 hours, and 72 hours resulted in a significant reduction of VEGF-A release by melanoma cells (C). The VEGF-A mRNA expression measured by real-time PCR was not affected by tinzaparin treatment of 48 hours (D). Bio-plex assays of different cell fractions showed a tinzaparin-induced reduction of VEGF-A in all fractions (E). Adding tinzaparin to Ret cell supernatant immediately before the measurements revealed an interaction of VEGF-A and tinzaparin (F). Binding of tinzaparin to VEGF-A was determined using the intrinsic tryptophan fluorescence (emission: 290 nm, excitation: 340 nm). The fluorescence of VEGF-A increases in a dose-dependent manner (G). In contrast to fondaparinux, tinzaparin exhibits a high binding affinity to VEGF-A (H). The binding of VEGF-A to tinzaparin inhibited VEGF-mediated ATP production of endothelial cells indicative for reduced cell proliferation (I). Data are presented as the mean ± SD of n = 4 of at least 2 independent experiments (*$P < .05$, **$P < .005$, ***$P < .001$; scale bars = 20 μm).

ret transgenic mice. As shown in Figure 4, melanoma-derived supernatant induced a prompt release of VWF through WPB exocytosis as shown by immunofluorescence analysis (Figure 4A) and ELISA (Figure 4B). Inhibition of Ret cell-derived VEGF-A by bevacizumab was sufficient to reduce ULVWF release to control levels, demonstrating the importance of melanoma-secreted VEGF-A for acute EC activation (Figure 4A-B). As treatment with bevacizumab has diverse side effects in tumor patients[28] and VEGF-A has a heparin binding site,[29] we used LMWH for inhibition of VEGF-A. The results show that the LMWH tinzaparin attenuated melanoma-induced EC activation (Figure 4B) and significantly reduced the level of Ret cell-secreted VEGF-A by 22% after 24 hours, by 32% after 48 hours, and 31% after 72 hours of incubation (Figure 4C). To exclude that incubation with tinzaparin alters the expression of VEGF-A, we performed real-time polymerase chain reaction (PCR) using total RNA from melanoma cells treated with tinzaparin for 48 hours or left untreated. The results clearly demonstrated that tinzaparin does not affect the expression of VEGF-A (Figure 4D). We next examined the effect of LMWHs on tumoral VEGF-A release by bio-plex assay (Figure 4E). Analysis of the eluted proteins demonstrated a tinzaparin-induced reduction of VEGF-A in the supernatant, in the cell lysate and the precipitated pellet. Because binding of tinzaparin to VEGF-A may affect the antibody recognition in the assay, we added tinzaparin to the supernatant of Ret cells immediately before the measurements. In accordance, reduced levels of measured VEGF-A indicate the interaction of VEGF-A and tinzaparin (Figure 4F). As final proof for this interaction, we applied a fluorescence-based method to analyze conformational changes upon protein-ligand binding. This method uses the intrinsic tryptophan fluorescence of a protein and ligand-induced changes of the solvent environment of tryptophan residues. Although the pentasaccharide fondaparinux revealed low binding affinity to VEGF-A (K_d= 296.2 ± 94.28 μM), tinzaparin binds to VEGF-A with high affinity in a concentration-dependent manner (K_d= 36.8 ± 11.02 μM) (Figure 4G-H). Of note, the data provide evidence for conformational changes of VEGF-A upon tinzaparin binding that modulate the activities of VEGF. Finally, the effect of heparin on endothelial cell proliferation was measured using ATP assays (Figure 4I). Compared with medium alone, recombinant VEGF-A increased cell proliferation by 15% which was blocked by addition of tinzaparin. Taken together, these results implicate that tumor-released VEGF-A accounts for EC activation and VWF fiber formation in the tumor vasculature. Tinzaparin binds to VEGF-A and thereby blocks its activity on melanoma-mediated EC activation.

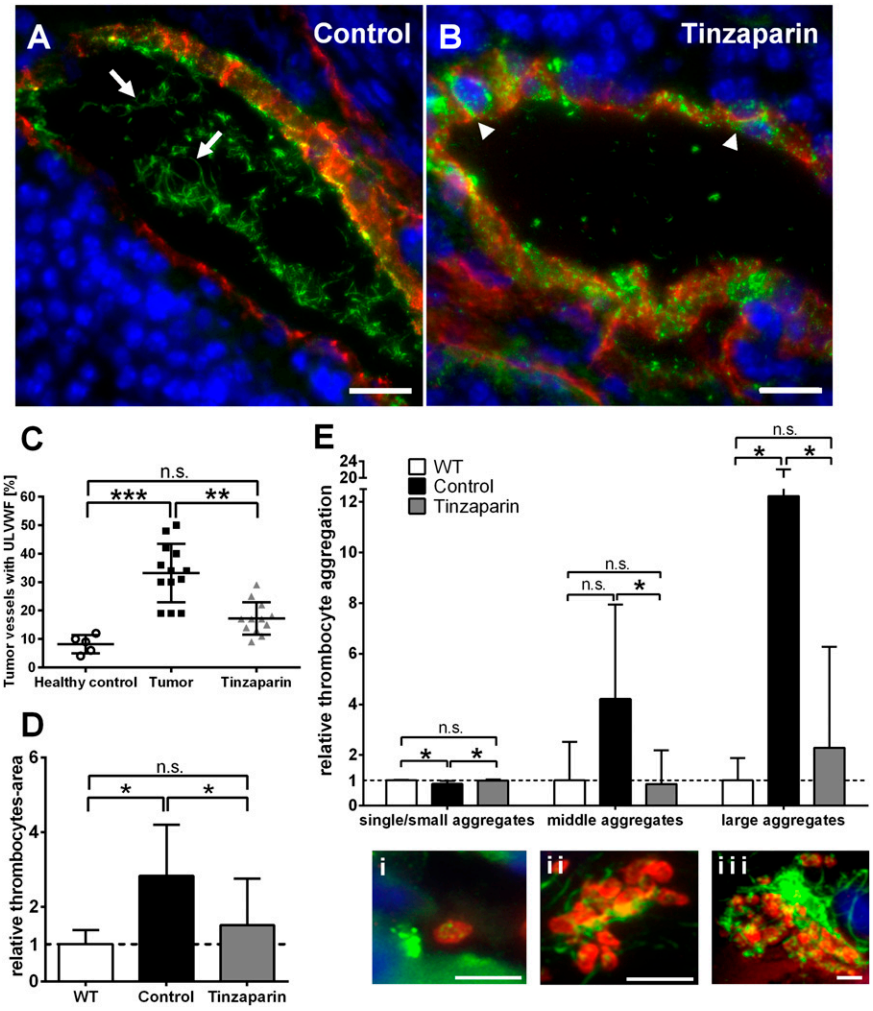

Figure 5. Blocking VEGF-A using tinzaparin reduces VWF fiber formation in tumor microvasculature. Immunofluorescence stainings for VWF (green) and anti-CD31 (red) in cryosections of *ret* transgenic tumors were performed. Nuclei were stained with DAPI. Tumor microvessels of control mice showed formation of ULVWF fibers in the vessel lumen (A, arrows). By contrast, microvessels of tinzaparin-treated mice showed almost no ULVWF fiber formation and a punctual pattern of VWF within the vessel wall (B, arrowheads), indicative of reduced endothelial cell activation. Representative pictures of tumor microvessels are shown (n = 10 animals of 2 independent experiments; scale bars = 20 μm). Tinzaparin treatment correlated with a significant reduction of vessels with intraluminal VWF fibers (C). Tumor vessels were analyzed for platelet aggregation using VWF (green) and GPIb (red) staining. Quantification showed a significant increase in platelet-covered area in the lumen of tumor vessels compared with control. This effect was abolished by treatment with tinzaparin (D-E). Panel Ei shows a single platelet in the lumen of a tumor blood vessel. In addition, the treatment of *ret* transgenic mice with tinzaparin (gray) reduced the appearance of middle (ii) and big aggregates (iii) to healthy control skin levels (white) compared with vehicle-treated control tumors (black). Plot shows mean ± SD (n = 5-10; $*P < .05$; $**P < .005$; $***P < .001$; scale bars = 5 μm).

Tinzaparin-induced inhibition of VEGF-A blocks EC activation in tumors

For in vivo proof of our findings, we treated *ret* transgenic mice with tinzaparin followed by analysis of microvessels and quantification of VWF fiber formation (Figure 5). As expected, the proportion of luminally released ULVWF in tumor microvessels was strongly increased in vehicle-treated tumors reflected by VWF fibers in the vessel lumen but reduced VWF staining in the vessel wall (Figure 5A arrows; supplemental Figure 3). In contrast, inhibition of tumor cell-secreted VEGF-A by tinzaparin increased VWF storage in the vessel wall (Figure 5B arrowheads; supplemental Figure 3) and intraluminal ULVWF formation was significantly reduced or even absent indicative for a decrease or inhibition of EC activation. Quantification revealed a significant reduction of tumor vessels with intraluminal ULVWF to 16.1% in tinzaparin-treated animals vs 32.9% in control tumors (Figure 5C; supplemental Table 1). As expected, a downregulation of intraluminal ULVWF fibers was accompanied by a reduction of intraluminal platelet count (Figure 5D) and inhibited VWF-mediated platelet aggregation in the lumen of tumor microvessels (Figure 5E).

Blocking EC activation by tinzaparin blocks tumor progression

We next asked whether inhibition of VEGF-A by tinzaparin and therefore VWF fiber formation affected metastasis formation in *ret* transgenic mice. To this end, we analyzed the distribution of the proliferation marker Ki67 in tumor cells of primary tumor tissue and lymph nodes (Figure 6). Within the tumors, we found a tinzaparin-induced reduction of proliferating tumor cells (Figure 6A-C). Flow cytometry using CD45.2 to exclude leukocytes identified 7.8% of cells as proliferating cancer cells in the tumor-bearing control group, whereas tinzaparin reduced the amount of malignant cells in the lymph nodes to 5% (Figure 6D). As our in vitro studies identified VEGF-A as potential target, we next analyzed the expression level of VEGF-A in skin tumors and lymph nodes. In accordance with in vitro results, the concentration of VEGF-A was dramatically reduced upon tinzaparin treatment vs control in skin melanomas (Figure 6E) and lymph nodes (Figure 6F). Interestingly, this effect decreased tumor weight by 30% and improved mouse survival in several independent experiments (Figure 6G-H; supplemental Video 1). Taken together, we conclude that an inhibition of tumor-released VEGF-A using tinzaparin attenuates EC activation, VWF fiber formation, and tumor progression upon a prolonged tinzaparin treatment schedule.

VEGF-A blockage reduces angiogenesis in intradermal tumors

Because VEGF-A is a strong promoter of angiogenesis,[1] we next analyzed the effect of tinzaparin treatment on localization of VEGF-A (supplemental Figure 4) and blood vessels using tumor sections of mouse melanomas (Figure 7). Treatment with tinzaparin slightly reduced VEGF-A staining (supplemental Figure 4) and according

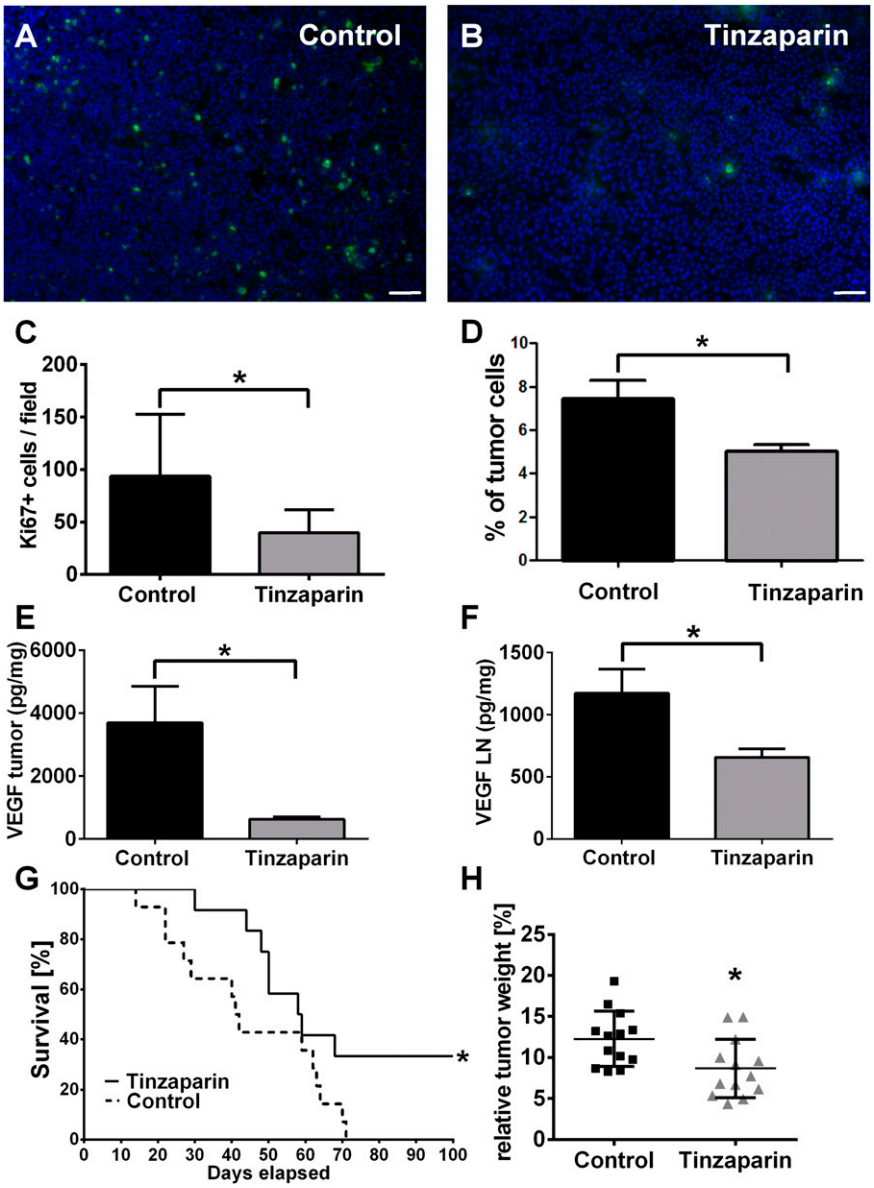

Figure 6. Tinzaparin attenuates proliferation of melanoma cells in primary tumor and lymph nodes and attenuates tumor progression in *ret* transgenic mice. Immunofluorescence stainings of tumor cell proliferation with Ki67 (green) and DAPI (nuclei, blue). Cryosections of vehicle-treated tumors (A) show more proliferating melanoma cells compared with tinzaparin-treated tumors (B; scale bars = 50 μm). Quantification showed a significant reduction of Ki67-positive cells after treatment with tinzaparin (C). Analysis of Ki67-positive tumor cells in lymph nodes of vehicle-treated *ret* mice and tinzaparin-treated animals was assessed by flow cytometry. Results show that tinzaparin induces a significant reduction of proliferating melanoma cells (D). Bars show mean ± SD (n = 7-10). Tumor-derived VEGF was measured in tumor and lymph nodes of *ret* transgenic mice (E-F) by bio-plex assay. VEGF levels were decreased in tumor samples (E) and lymph nodes (F) after treatment with tinzaparin (n = 5-7 different mice each group). Consequently, a survival benefit (G) and a reduced tumor weight (H) compared with vehicle-treated control was observed after tinzaparin treatment (n = 13 of 2 independent experiments). Plot shows mean ± SD; $*P < .05$. See also supplemental Video 1.

to the staining of $CD31^+$ vessels, the LMWH significantly reduced the vascular area by 20% compared with vehicle control (Figure 7C). This was reflected by a relative increase of small vessels (<50 μm) and a reduction of big blood vessels (>150 μm) providing direct evidence of antiangiogenic effects of VEGF-A inhibition by binding to tinzaparin (Figure 7D).

Discussion

Since the pioneering work by Moake et al in 1982, it is postulated that ULVWF fibers exist in patients suffering from TTP.[30] These ULVWF multimers detected by gel electrophoresis were shown to be responsible for the life-threatening occlusion of microvessels mainly within the brain, kidney, and heart,[31-33] predisposing to an increased risk of cardiovascular diseases.[34] Consistent with this, a deficiency or dysfunction of VWF causes the bleeding disorder von Willebrand disease (type 1-3).[35] Under physiological conditions, ADAMTS13 specifically cleaves these ULVWF fibers into smaller fragments, thus downregulating the hemostatic activity of VWF.[36] Therefore, missing ADAMTS13 activity, by neutralizing autoantibodies or by reduced protein expression, represents the pathophysiological correlate for TTP and the appearance of ULVWF multimers in those patients.[37-39] However, since 1982, the formation of these ULVWF multimers has never been shown in human vessels.

Here, we show ULVWF network formation in the microvasculature of malignant melanoma of mice and humans (Figures 1 and 2). In strong accordance, we and others previously reported the generation of ULVWF fibers in vitro.[9,40,41] However, this effect was restricted to the absence or inhibition of ADAMTS13 in these in vitro settings.[42] As it is postulated that ULVWF fibers may only occur by profound EC activation combined with absence of ADAMTS13 activity,[25,43-45] we postulate local inhibition or deficiency of ADAMTS13 activity in tumor vessels. The following arguments support our hypothesis: our own studies demonstrated that melanoma cells activate ECs,[3-5] followed by a profound release of VWF fibers, and may therefore

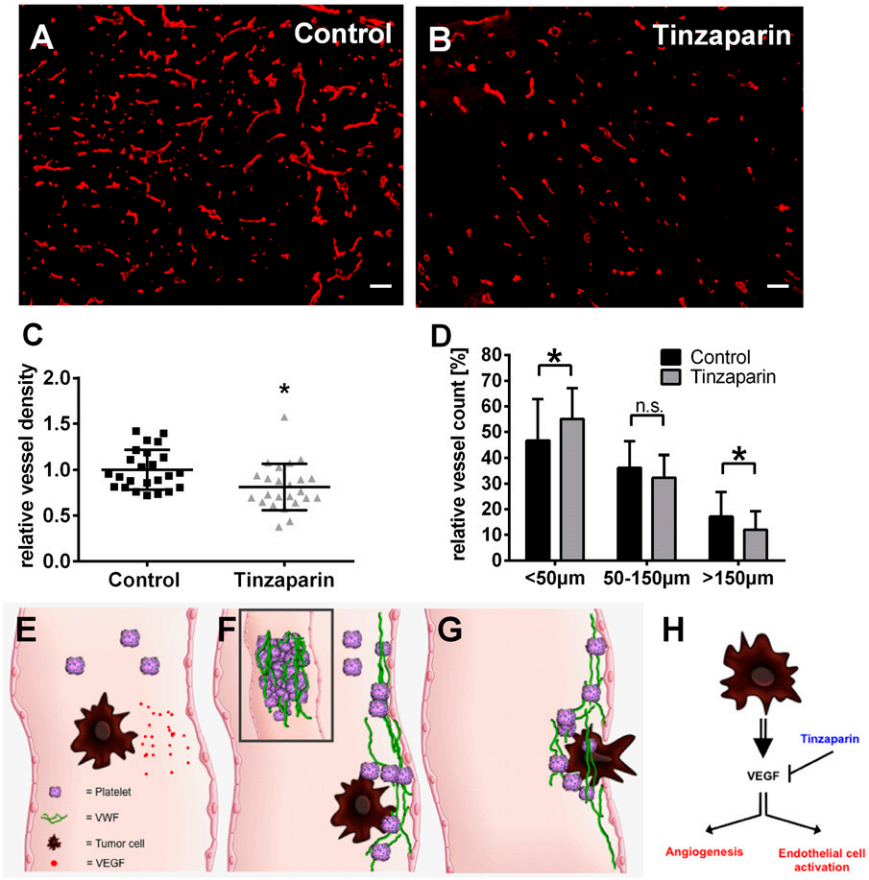

Figure 7. Tinzaparin inhibits VEGF-A–mediated angiogenesis in primary skin tumors and impedes tumor cell metastasis. Tumor-bearing mice were treated with vehicle (A; control) or tinzaparin (B) and cryosections of primary tumors were analyzed by immunofluorescences for CD31. Morphometric quantification of the vessel density (C) demonstrates a significant difference in vessel density upon tinzaparin treatment compared with control tumors. Quantitative assessment of vessels in tinzaparin-treated tumors (D) shows that tinzaparin treatment results in a significant increase of small vessels (<50 μm) and decrease of big vessels (>150 μm). Plots show mean ± SD (n = 4-6 animals of 2 independent experiments; scale bar = 100 μm; *$P < .05$). Schematic overview shows the role of tumor cell-mediated EC activation in cancer progression (E-G). Circulating tumor cells secrete VEGF (E) followed by activation of endothelial cells and the release of procoagulatory VWF fibers (F). VWF mediates platelet aggregation and tumor cell binding, promoting extravasation (G). Binding of the LMWH tinzaparin blocks VEGF-mediated angiogenesis and VWF release attenuating tumor progression (H).

imbalance the ratio between ADAMTS13 and ULVWF fibers. Notably, in this study, we identified VEGF-A as a strong promoter of EC activation accompanied by ULVWF release in tumor microvessels (Figures 2 and 4). Furthermore, our human studies showed elevated levels of TNF-α, IFN-γ, and IL-6 (Figure 2), cytokines known to inhibit ADAMTS13 activity and expression.[26,27] These findings are in line with a strong increase of TNF-α, IL-6, and IFN-γ in malignant melanoma tumors of *ret* transgenic mice.[20,22,46,47] Moreover, reconstitution of ADAMTS13 by infusion of the recombinant enzyme counteracts ULVWF network formation in tumor microvessels. In strong accordance, the proteolytic activity and the protein concentration of ADAMTS13 are decreased in tumor tissue (Figure 3; supplemental Table 2). Thus, a high amount of EC-derived ULVWF mediated by tumor-derived VEGF-A and reduced ADAMTS13 activity is a sound explanation for the observed formation of ULVWF fibers within tumor microvasculature.

An important finding of this study is that EC-released VWF fibers markedly bind platelets (Figures 1 and 2). Of note, earlier experiments addressed the relevance of platelets in metastasis.[14] Platelet aggregates may protect cancer cells from immune cells, such as natural killer cells,[12,48] or may directly influence tumor extravasation as the platelet-derived factors VEGF-A, thrombin, and platelet-activating factor activate ECs.[49-51] Finally, we previously showed in mouse models that leukocyte extravasation in mesenteric vessels is dependent on VWF-mediated permeability.[52,53] This step could be related to vascular dissemination of cancer cells facilitated by VWF-recruited platelets mediating vascular permeability and tumor-associated activation of the coagulation.

Obviously, an increasing body of evidence indicates that treatment with LMWHs such as tinzaparin is not only suitable to prevent cancer-associated thrombosis, but is also a potential antiagent for therapeutic use.[54,55] In our own study, tinzaparin treatment, upon tumor onset, improves survival and attenuates tumor progression in the *ret* mouse model (Figures 5 and 6). In contrast to most tumor models, the *ret* transgenic mouse model closely resembles the clinical situation of melanoma patients with metastasis in lymph nodes, lungs, and brain.[20-22]

Due to its complex composition, a plethora of potential mechanisms for heparin effects on metastasis are discussed. Next to interaction with heparanase, enzymes, and growth factors, most studies suggest selectins as a main target of heparins.[29,55] However, P-selectin mediating the adhesion of tumor cells to the vascular endothelium is exposed to the EC surface upon activation only.[56] Because all previous studies lack the explanation of mechanisms involved in EC activation that is needed to expose P-selectin, the results from the present study strengthen the idea that tinzaparin blocks EC activation via binding to VEGF-A. The LMWH binds to the growth factor and reduces VEGF-A–mediated release of ULVWF (Figures 4 and 6) and angiogenesis (Figure 7). Indeed, heparin contains a growth factor binding site[57] and our VEGF-A has been identified as main mediator of angiogenesis[1,58] and a strong inducer of EC activation[4] promoting cancer progression. Thus, tumor cell-secreted VEGF-A may facilitate cancer cell extravasation and hypercoagulation through EC activation and VWF fiber generation mediating platelet aggregation and the binding of tumor cells to the vessel wall (Figure 7E-G).

On the basis of these findings, an anti-VEGF strategy seems to be promising to treat patients with metastatic melanoma.[59] However, the angiogenesis inhibitor bevacizumab has diverse side effects and enhances the risk of hypercoagulation.[28,60,61] VEGF blockage provokes endothelial apoptosis and may mediate coagulatory processes via platelet binding to damaged tissue.[61] Therefore, heparins may represent antithrombotic and innovative therapeutic targets for cancer treatment.

Taken together, our data propose a new mechanism of tumor-related procoagulatory activity that indicates the impact of ADAMTS13 and VWF in thrombotic microangiopathies other than TTP. It is tempting to speculate that this mechanism could be relevant for other pathophysiological conditions, such as autoinflammatory diseases and sepsis, known to support the formation of ULVWF fibers and attenuate ADAMTS13 activity.[31,33,62-64]

Thus, our data provide essential information delineating thrombotic mechanisms and highlight EC activation or microthrombi formation as new therapeutic targets in cancer treatment (Figure 7H).

Acknowledgments

The authors thank Natalia Halter and Sayran Arif-Said for excellent technical help and Birgit Schneider for artwork in Figure 7.

This work was supported by the Deutsche Forschungsgemeinschaft within the RTG2099 (A.T.B., S.W.S.), SFB/Transregio 23 (project A9 [S.W.S.], C6 [M.H.]), project SCHN 474/5-1 (S.W.S), GO1360/4-1 (T.G.), the German Cancer Aid (J.U.), and the Initiative and Networking Fund of the Helmholtz Association within the Helmholtz Alliance on Immunotherapy of Cancer (V.U.).

Authorship

Contribution: A.T.B. and J.S. wrote the manuscript and contributed to all experiments; K.F., N.D.-V. C.G., A.D., L.G., L.U., and P.B. performed experiments and generated data; A.H.W., M.H., J.U., T.G., and V.U. analyzed and discussed data; and the study was conceived and supervised by S.W.S.

Conflict-of-interest disclosure: The authors declare no competing financial interests.

Correspondence: Stefan W. Schneider, Medical Faculty Mannheim, University of Heidelberg, Theodor-Kutzer-Ufer 1-3, Mannheim, 68167 Germany; e-mail: stefan.schneider@medma.uni-heidelberg.de.

References

1. Steeg PS. Tumor metastasis: mechanistic insights and clinical challenges. *Nat Med.* 2006; 12(8):895-904.
2. Wolf MJ, Hoos A, Bauer J, et al. Endothelial CCR2 signaling induced by colon carcinoma cells enables extravasation via the JAK2-Stat5 and p38MAPK pathway. *Cancer Cell.* 2012;22(1): 91-105.
3. Kerk N, Strozyk EA, Pöppelmann B, Schneider SW. The mechanism of melanoma-associated thrombin activity and von Willebrand factor release from endothelial cells. *J Invest Dermatol.* 2010;130(9):2259-2268.
4. Desch A, Strozyk EA, Bauer AT, et al. Highly invasive melanoma cells activate the vascular endothelium via an MMP-2/integrin αvβ5-induced secretion of VEGF-A. *Am J Pathol.* 2012;181(2): 693-705.
5. Goerge T, Barg A, Schnaeker EM, et al. Tumor-derived matrix metalloproteinase-1 targets endothelial proteinase-activated receptor 1 promoting endothelial cell activation. *Cancer Res.* 2006;66(15):7766-7774.
6. Wagner DD, Frenette PS. The vessel wall and its interactions. *Blood.* 2008;111(11):5271-5281.
7. Reininger AJ. Function of von Willebrand factor in haemostasis and thrombosis. *Haemophilia.* 2008;14(suppl 5):11-26.
8. Ruggeri ZM. Platelets in atherothrombosis. *Nat Med.* 2002;8(11):1227-1234.
9. Schneider SW, Nuschele S, Wixforth A, et al. Shear-induced unfolding triggers adhesion of von Willebrand factor fibers. *Proc Natl Acad Sci USA.* 2007;104(19):7899-7903.
10. Goerge T, Kleinerüschkamp F, Barg A, et al. Microfluidic reveals generation of platelet-strings on tumor-activated endothelium. *Thromb Haemost.* 2007;98(2):283-286.
11. Brill A, Fuchs TA, Chauhan AK, et al. von Willebrand factor-mediated platelet adhesion is critical for deep vein thrombosis in mouse models. *Blood.* 2011;117(4):1400-1407.
12. Menter DG, Tucker SC, Kopetz S, Sood AK, Crissman JD, Honn KV. Platelets and cancer: a casual or causal relationship: revisited. *Cancer Metastasis Rev.* 2014;33(1):231-269.
13. Schumacher D, Strilic B, Sivaraj KK, Wettschureck N, Offermanns S. Platelet-derived nucleotides promote tumor-cell transendothelial migration and metastasis via P2Y2 receptor. *Cancer Cell.* 2013;24(1):130-137.
14. Erpenbeck L, Schön MP. Deadly allies: the fatal interplay between platelets and metastasizing cancer cells. *Blood.* 2010;115(17):3427-3436.
15. Sørensen HT, Mellemkjaer L, Olsen JH, Baron JA. Prognosis of cancers associated with venous thromboembolism. *N Engl J Med.* 2000;343(25): 1846-1850.
16. Dammacco F, Vacca A, Procaccio P, Ria R, Marech I, Racanelli V. Cancer-related coagulopathy (Trousseau's syndrome): review of the literature and experience of a single center of internal medicine. *Clin Exp Med.* 2013;13(2): 85-97.
17. Pabinger I, Thaler J, Ay C. Biomarkers for prediction of venous thromboembolism in cancer. *Blood.* 2013;122(12):2011-2018.
18. Sparsa A, Durox H, Doffoel-Hantz V, et al. High prevalence and risk factors of thromboembolism in stage IV melanoma. *J Eur Acad Dermatol Venereol.* 2011;25(3):340-344.
19. Kakkar AK, Macbeth F. Antithrombotic therapy and survival in patients with malignant disease. *Br J Cancer.* 2010;102(suppl 1):S24-S29.
20. Kato M, Takahashi M, Akhand AA, et al. Transgenic mouse model for skin malignant melanoma. *Oncogene.* 1998;17(14):1885-1888.
21. Umansky V, Abschuetz O, Osen W, et al. Melanoma-specific memory T cells are functionally active in Ret transgenic mice without macroscopic tumors. *Cancer Res.* 2008;68(22): 9451-9458.
22. Zhao F, Falk C, Osen W, Kato M, Schadendorf D, Umansky V. Activation of p38 mitogen-activated protein kinase drives dendritic cells to become tolerogenic in ret transgenic mice spontaneously developing melanoma. *Clin Cancer Res.* 2009; 15(13):4382-4390.
23. Kimpfler S, Sevko A, Ring S, et al. Skin melanoma development in ret transgenic mice despite the depletion of CD25+Foxp3+ regulatory T cells in lymphoid organs. *J Immunol.* 2009;183(10): 6330-6337.
24. Mannucci PM, Canciani MT, Forza I, Lussana F, Lattuada A, Rossi E. Changes in health and disease of the metalloprotease that cleaves von Willebrand factor. *Blood.* 2001;98(9):2730-2735.
25. Coppo P, Schwarzinger M, Buffet M, et al; French Reference Center for Thrombotic Microangiopathies. Predictive features of severe acquired ADAMTS13 deficiency in idiopathic thrombotic microangiopathies: the French TMA reference center experience. *PLoS ONE.* 2010; 5(4):e10208.
26. Cao WJ, Niiya M, Zheng XW, Shang DZ, Zheng XL. Inflammatory cytokines inhibit ADAMTS13 synthesis in hepatic stellate cells and endothelial cells. *J Thromb Haemost.* 2008;6(7):1233-1235.
27. Bernardo A, Ball C, Nolasco L, Moake JF, Dong JF. Effects of inflammatory cytokines on the release and cleavage of the endothelial cell-derived ultralarge von Willebrand factor multimers under flow. *Blood.* 2004;104(1):100-106.
28. Kamba T, McDonald DM. Mechanisms of adverse effects of anti-VEGF therapy for cancer. *Br J Cancer.* 2007;96(12):1788-1795.
29. Norrby K. Low-molecular-weight heparins and angiogenesis. *APMIS.* 2006;114(2):79-102.
30. Moake JL, Rudy CK, Troll JH, et al. Unusually large plasma factor VIII:von Willebrand factor multimers in chronic relapsing thrombotic thrombocytopenic purpura. *N Engl J Med.* 1982; 307(23):1432-1435.
31. Motto D. Endothelial cells and thrombotic microangiopathy. *Semin Nephrol.* 2012;32(2): 208-214.
32. Moake JL. Thrombotic microangiopathies. *N Engl J Med.* 2002;347(8):589-600.
33. Sadler JE. Von Willebrand factor, ADAMTS13, and thrombotic thrombocytopenic purpura. *Blood.* 2008;112(1):11-18.
34. Spiel AO, Gilbert JC, Jilma B. von Willebrand factor in cardiovascular disease: focus on acute coronary syndromes. *Circulation.* 2008;117(11): 1449-1459.
35. Lillicrap D. von Willebrand disease: advances in pathogenetic understanding, diagnosis, and therapy. *Blood.* 2013;122(23):3735-3740.
36. Zhang X, Halvorsen K, Zhang CZ, Wong WP, Springer TA. Mechanoenzymatic cleavage of the ultralarge vascular protein von Willebrand factor. *Science.* 2009;324(5932):1330-1334.
37. Levy GG, Nichols WC, Lian EC, et al. Mutations in a member of the ADAMTS gene family cause thrombotic thrombocytopenic purpura. *Nature.* 2001;413(6855):488-494.
38. Veyradier A, Obert B, Houllier A, Meyer D, Girma JP. Specific von Willebrand factor-cleaving

protease in thrombotic microangiopathies: a study of 111 cases. *Blood.* 2001;98(6):1765-1772.

39. Feys HB, Roodt J, Vandeputte N, et al. Inhibition of von Willebrand factor-platelet glycoprotein Ib interaction prevents and reverses symptoms of acute acquired thrombotic thrombocytopenic purpura in baboons. *Blood.* 2012;120(17): 3611-3614.
40. Barg A, Ossig R, Goerge T, et al. Soluble plasma-derived von Willebrand factor assembles to a haemostatically active filamentous network. *Thromb Haemost.* 2007;97(4):514-526.
41. Dong JF, Moake JL, Nolasco L, et al. ADAMTS-13 rapidly cleaves newly secreted ultralarge von Willebrand factor multimers on the endothelial surface under flowing conditions. *Blood.* 2002; 100(12):4033-4039.
42. De Ceunynck K, De Meyer SF, Vanhoorelbeke K. Unwinding the von Willebrand factor strings puzzle. *Blood.* 2013;121(2):270-277.
43. Moake JL. von Willebrand factor, ADAMTS-13, and thrombotic thrombocytopenic purpura. *Semin Hematol.* 2004;41(1):4-14.
44. Chauhan AK, Goerge T, Schneider SW, Wagner DD. Formation of platelet strings and microthrombi in the presence of ADAMTS-13 inhibitor does not require P-selectin or beta3 integrin. *J Thromb Haemost.* 2007;5(3):583-589.
45. Claus RA, Bockmeyer CL, Budde U, et al. Variations in the ratio between von Willebrand factor and its cleaving protease during systemic inflammation and association with severity and prognosis of organ failure. *Thromb Haemost.* 2009;101(2):239-247.
46. Meyer C, Sevko A, Ramacher M, et al. Chronic inflammation promotes myeloid-derived suppressor cell activation blocking antitumor immunity in transgenic mouse melanoma model. *Proc Natl Acad Sci USA.* 2011;108(41): 17111-17116.
47. Sevko A, Michels T, Vrohlings M, et al. Antitumor effect of paclitaxel is mediated by inhibition of myeloid-derived suppressor cells and chronic inflammation in the spontaneous melanoma model. *J Immunol.* 2013;190(5):2464-2471.
48. Quail DF, Joyce JA. Microenvironmental regulation of tumor progression and metastasis. *Nat Med.* 2013;19(11):1423-1437.
49. Siegel-Axel DI, Gawaz M. Platelets and endothelial cells. *Semin Thromb Hemost.* 2007; 33(2):128-135.
50. Ostrovsky L, King AJ, Bond S, et al. A juxtacrine mechanism for neutrophil adhesion on platelets involves platelet-activating factor and a selectin-dependent activation process. *Blood.* 1998;91(8): 3028-3036.
51. Battinelli EM, Markens BA, Kulenthirarajan RA, Machlus KR, Flaumenhaft R, Italiano JE Jr. Anticoagulation inhibits tumor cell-mediated release of platelet angiogenic proteins and diminishes platelet angiogenic response. *Blood.* 2014;123(1):101-112.
52. Petri B, Broermann A, Li H, et al. von Willebrand factor promotes leukocyte extravasation. *Blood.* 2010;116(22):4712-4719.
53. Hillgruber C, Steingraber AK, Poppelmann B, et al. Blocking von Willebrand factor for treatment of cutaneous inflammation. *J Invest Dermatol.* 2014;134(1):77-86.
54. Nicolaides A, Hull RD, Fareed J; Cardiovascular Disease Educational and Research Trust; European Venous Forum; North American Thrombosis Forum; International Union of Angiology and Union Internationale du Phlebologie. Treatment for patients with cancer. *Clin Appl Thromb Hemost.* 2013;19(2):206-208.
55. Borsig L. Antimetastatic activities of heparins and modified heparins. Experimental evidence. *Thromb Res.* 2010;125(suppl 2):S66-S71.
56. Cleator JH, Zhu WQ, Vaughan DE, Hamm HE. Differential regulation of endothelial exocytosis of P-selectin and von Willebrand factor by protease-activated receptors and cAMP. *Blood.* 2006; 107(7):2736-2744.
57. Norrby K, Nordenhem A. Dalteparin, a low-molecular-weight heparin, promotes angiogenesis mediated by heparin-binding VEGF-A in vivo. *APMIS.* 2010;118(12):949-957.
58. Neufeld G, Cohen T, Gengrinovitch S, Poltorak Z. Vascular endothelial growth factor (VEGF) and its receptors. *FASEB J.* 1999;13(1):9-22.
59. Schuster C, Eikesdal HP, Puntervoll H, et al. Clinical efficacy and safety of bevacizumab monotherapy in patients with metastatic melanoma: predictive importance of induced early hypertension. *PLoS ONE.* 2012;7(6): e38364.
60. Nalluri SR, Chu D, Keresztes R, Zhu X, Wu S. Risk of venous thromboembolism with the angiogenesis inhibitor bevacizumab in cancer patients: a meta-analysis. *JAMA.* 2008;300(19): 2277-2285.
61. Yang Y, Zhang Y, Cao Z, et al. Anti-VEGF- and anti-VEGF receptor-induced vascular alteration in mouse healthy tissues. *Proc Natl Acad Sci USA.* 2013;110(29):12018-12023.
62. Bockmeyer CL, Claus RA, Budde U, et al. Inflammation-associated ADAMTS13 deficiency promotes formation of ultra-large von Willebrand factor. *Haematologica.* 2008;93(1):137-140.
63. Pappelbaum KI, Gorzelanny C, Grässle S, et al. Ultralarge von Willebrand factor fibers mediate luminal Staphylococcus aureus adhesion to an intact endothelial cell layer under shear stress. *Circulation.* 2013;128(1):50-59.
64. Bridges DJ, Bunn J, van Mourik JA, et al. Rapid activation of endothelial cells enables Plasmodium falciparum adhesion to platelet-decorated von Willebrand factor strings. *Blood.* 2010;115(7):1472-1474.